INFLUENCE OF PULSATION FREQUENCIES ON THE HEAT TRANSFER IN LAMINAR FREE SURFACE JET IMPINGEMENT

Ehrenpreis C.*, Sabelberg E., Kneer R. and Rohlfs W.
*Author for correspondence
Institute of Heat and Mass Transfer,
RWTH Aachen university,
Augustinerbach 6,
52062 Aachen,
Germany,
E-mail: ehrenpreis@wsa.rwth-aachen.de

ABSTRACT

This study aims to describe the influence of periodic flow-pulsations on heat transfer of laminar free surface impinging jets ($\overline{Re} = 1000$, $Pr = 7$). Fully resolved two-dimensional numerical simulations were carried out in which flow-pulsation was achieved by periodically altering the velocity of the jet at the nozzle exit with an amplitude of 50% of the time averaged value. The Strouhal number of this pulsation was varied between $St = 0.002 - 0.2$. For higher pulsation frequencies, linked to higher Strouhal numbers, the time averaged Nusselt number in the stagnation region shows an increase compared to the Nusselt number of a non-pulsating jet, while it decreases for lower pulsation frequencies. The physical effects causing these two regimes are described analytically and it is shown that the resulting correlations can deliver lower and upper limits for the deviation from the Nusselt number distribution of non pulsating jets.

INTRODUCTION

Impinging jets show, due to the high transport rates at the target wall, a high potential for cooling and drying processes and are already broadly implemented in such applications [1][2]. The heat and mass transfer characteristics of jets have been investigated in various publications. A overview over the heat transfer in laminar jets was presented by Kneer et al. [3] while Jambunathan et al.[4] and more recently Dewan et al. [5] give and overview over the research regarding turbulent submerged jets and Ma et al. [6] summarises the research on laminar and turbulent free surface jets.

The affect of unsteady flow behaviour on the heat transfer of submerged laminar jets has previously been investigated by the authors of this work, see Rohlfs et al. [7] [8] as well as Liu and Sullivan [9], Chung and Luo [10] and Hofmann [11]. A common finding of these investigations was that in submerged jets, large vortices which are induced at the outer edge of the jet can substantially affect the local instantaneous and time averaged heat transfer coefficients.

NOMENCLATURE

A	$[-]$	pulsation amplitude
D	$[\mathrm{m}]$	jet diameter
ν	$[\mathrm{m^2/s}]$	kinematic viscosity of the jets fluid
ω	$[1/\mathrm{s}]$	pulsation frequency
$\dot{P}$	$[\mathrm{kg \cdot m/s^2}]$	momentum flux of the jet
q''	$[\mathrm{W/m^2}]$	heat flux
r	$[\mathrm{m}]$	radial coordinate
Δr	$[\mathrm{m}]$	radial cell measure
ρ	$[\mathrm{kg/m^3}]$	density of the jets fluid
t	$[\mathrm{s}]$	physical time
Δt	$[\mathrm{s}]$	pulsation length of the inlet velocity
θ	$[\mathrm{K}]$	heat flux
u	$[\mathrm{m/s}]$	velocity
x	$[\mathrm{m}]$	axial coordinate
Δx	$[\mathrm{m}]$	axial cell measure

Dimensionless Numbers

Nu	$h \cdot D/\lambda$	Nusselt number
Pr	$\nu \cdot \rho \cdot D/\lambda$	Prandtl number of the jets fluid
Re	$u_{in,A} \cdot D/\nu$	Reynolds number
St	$\omega \cdot D/2\pi \cdot u_{in,A}$	Strouhal number

Subscripts

A	area averaged value
in	inlet value
N	values of non pulsating jets
P	values of pulsating jets
w	value on the target wall

The two-phase nature of free jets prevents the formation of such vortices within the jet. Nevertheless Zumbrunnen and Aziz [12] and Sheriff and Zumbrunnen [13] found that flow pulsation or intermittency can have an impact on the local heat transfer in planar turbulent impinging jets. While intermittent jets as well as a square-pulse-excitation showed an increase in heat transfer by a factor from 30 % up to 100 %, a sinusoidal pulsation led to a decrease up to 17 %, depending on the pulsation frequency. Sabelberg et al. [14] investigated various methods to passively induce pulsation in free surface jets.

NUMERICAL PROCEDURE

The simulations are carried out using a modified version of the *interFoam*-solver from the *OpenFOAM-1.7*-library [17]. It utilizes the Volume-Of-Fluid method (VOF) to model the

two-phase nature of the fluid flow and additionally incorporates the thermal energy transport equation in order to simulate the heat transport inside the fluid. A more detailed documentation of the numerical methods can be found in Rohlfs et al. [18].

In order to decrease the numerical costs of this investigation, it was taken advantage of the symmetric nature of the circular laminar impinging flow. This way, the numerical domain can be reduced to a two-dimensional radialy-symmetrical numerical mesh. The size of the numerical grid-cells is constant in radial direction with a resolution of $\Delta r/D = 5 \times 10^{-3}$. In axial direction the cell size is refined in five steps from a maximum size of $\Delta x/D \approx 9.5 \times 10^{-3}$ in the outer flow to a minimum size $\Delta x/D \approx 3 \times 10^{-4}$ close to the target wall. The grid independence of the results for such a numerical grid has been shown by the authors in Rohlfs et al. [18].

At the inlet of the numerical domain a fixed velocity boundary condition was applied, the values and distribution of which correspond to a parabolic velocity profile as it develops in laminar pipe flows. As the incoming jet is pulsating in a sinusoidal manner, the local velocity not only depends on the radial position but also on time, according to the equation

$$u_{in}(r,t) = 2 \cdot \overline{u}_{in,A} \cdot \left(1 - \frac{4 \cdot r^2}{D^2}\right) \cdot (1 + A \cdot sin(\omega \cdot t)) \qquad (1)$$

where $A = u'_{in}/\overline{u}_{in,A}$ is the relative pulsation amplitude and $\overline{u}_{in,A}$ is the time and area averaged jet velocity calculated from the time averaged volume flux $\overline{\dot{V}}$ according to

$$\overline{u}_{in,A} = \frac{4 \cdot \overline{\dot{V}}}{\pi D^2} = \frac{4}{\pi D^2 \Delta t} \int_0^{\Delta t} \dot{V}(t) \mathrm{d}t \; . \qquad (2)$$

The term $\Delta t = 2\pi/\omega$ denotes the sinus-pulsation length of the velocity at the inlet. The average Reynolds number of the jet is defined using this average velocity $\overline{u}$ and the jet diameter D according to

$$\overline{Re} = \frac{\overline{u}_{in,A} \cdot D}{\nu} \; . \qquad (3)$$

In addition to the time averaged Reynolds number $\overline{Re}$, the instantaneous Reynolds number $Re(t)$ which depends on the time dependent area averaged inlet velocity $u_{in,A}(t)$ can be defined analogue to Equation 2 and Equation 3

$$Re(t) = \frac{u_{in,A}(t) \cdot D}{\nu} \qquad (4)$$

with the instantaneous area averaged inlet velocity

$$u_{in,A}(t) = \overline{u}_{in,A} \cdot (1 + A \cdot sin(\omega \cdot t)) \; . \qquad (5)$$

The pulsation frequency is defined in non-dimensional form through the Strouhal number

$$St = \frac{f \cdot D}{\overline{u}_{in,A}} = \frac{\omega \cdot D}{2\pi \cdot \overline{u}_{in,A}} \; . \qquad (6)$$

In the following, jets with a comparably high Strouhal number and hence a high pulsation frequency will be referred to as fast pulsating jets, while jets with a low Strouhal number will be referred to as slowly pulsating jets.

At the solid wall a no-slip boundary condition is applied, whilst at the outlet a inlet-outlet condition is applied which couples an inward flow with the pressure gradient while for an outgoing flow a zero-gradient condition is applied. For the pressure field a fixed value is set as the boundary condition at the outlet patch. At all other patches a zero-gradient is applied. The alpha field which describes the volume fraction of the two phases in the VOF-method has a zero-gradient condition at the outlet and the wall and a fixed value at the inlet.

The heat transfer can be described in a non-dimensional form through the Nusselt number

$$Nu(r,t) = \frac{h(r,t) \cdot D}{\lambda} \; . \qquad (7)$$

Since the heat transfer coefficient $h(r,t)$ heavily depends on the non-stationary flow state, the Nusselt number is not only a function of the radial position but also a function of time. As this work aims to investigate the effect of pulsating flow on the average heat transfer, the time averaged Nusselt number is defined according to the definition suggested by Mladin and Zumbrunnen [19] as

$$\overline{Nu}(r) = \frac{\int_0^{\Delta t} Nu(r,t) \cdot \theta_w(r,t) \mathrm{d}t}{\int_0^{\Delta t} \theta_w(r,t) \mathrm{d}t} = \frac{D \cdot q''_w}{\lambda \cdot \overline{\theta}_w(r)} = \frac{D \cdot \overline{h}(r)}{\lambda} \qquad (8)$$

where the local wall temperature $\theta_w(r,t) = T_w(r,t) - T_{in}$ is used as scaling factor. Since in this investigation, a Neumann boundary condition is applied for the temperature field at the wall, the heat flux q''_w is spatially and temporarily constant.

RESULTS

Figure 1 shows the radial distribution of the time averaged Nusselt number for pulsating jets with different Strouhal numbers and a Prandtl number of $Pr = 7$. The black lines represent the reference distribution which would occur for jets without pulsation while the coloured lines are the time averaged results for pulsating jets. All pulsating jets have the same average Reynolds number $\overline{Re} = 1000$ and relative pulsation amplitude $A = 0.5$ but vary in pulsation frequency, with Strouhal numbers

ranging from $St = 0.02$ to $St = 0.2$. The pulsation amplitude leads to instantaneous Reynolds numbers ranging from $500 \leq Re(t) \leq 1500$. Hence the dashed black lines show the Nusselt number distribution of jets with such Reynolds numbers. The time averaged Nusslet number shows a distinct dependency on the Strouhal number, with higher Strouhal numbers leading to higher Nusselt numbers within the stagnation region. For the jet with the highest Strouhal number the heat transfer is increased compared to the non-pulsating jet, while in the other cases the heat transfer is impaired.

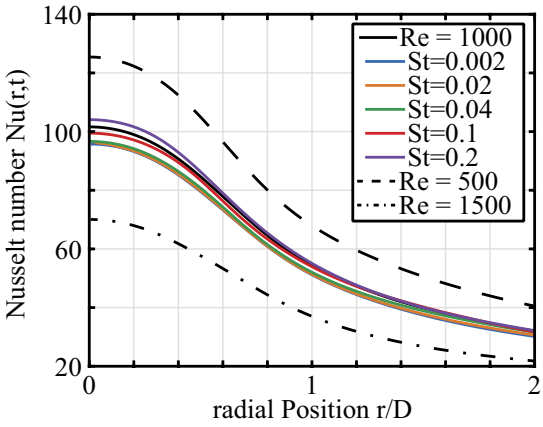

Figure 1: Time averaged Nusselt number distribution over radial position, for non-pulsating (black lines) and pulsating jets (coloured lines) with a parabolic inlet-velocity-profile.

Figure 2 and Figure 3 provide an explanation for the significant differences in the Nusselt number distributions for jets with high and low Strouhal numbers. Both graphs show Nusselt number distributions at constant time intervals within one pulsation period for a fast pulsating jet (Figure 3, $St = 0.2$) and a slowly pulsating jet (Figure 2, $St = 0.002$). In addition, three non-pulsating jets with the corresponding average and bounding Reynolds numbers ($Re_{min} = 500$, $\overline{Re} = 1000$, $Re_{max} = 1500$) of the pulsating jet are presented (black lines).

In both cases the variation of the Nusselt number at different time steps is strongest close to the stagnation point and vanishes for higher radial positions. While the slow pulsating jet shows a large spread between the Nusselt numbers at different time steps, the Nusselt numbers of the fast pulsating vary less and only in the stagnation region ($r/D \leq 0.5$). In the case of the slowly pulsating jet they reach the upper and lower bounds set by the bounding distributions of the non pulsating jets ($Re_{min} = 500$ and $Re_{max} = 1500$).

Figure 4 compares the time dependency of the stagnation point Nusselt number ($Nu(r = 0,t)$) with the wall shear stress at the radial position $r = 1 \times D$ for the two pulsating-jet cases shown in Figure 2 and Figure 3. It shows that even though the pulsation amplitude of the incoming jet is the same in both cases

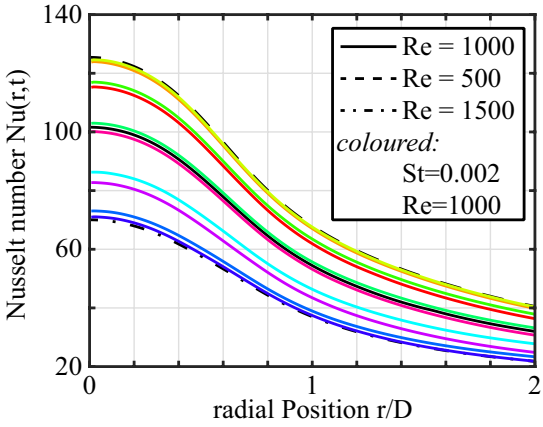

Figure 2: Nusselt number distribution over radial position, for non-pulsating (black lines), instantaneous Nusselt number distributions for a pulsating jet St=0.002 (coloured lines).

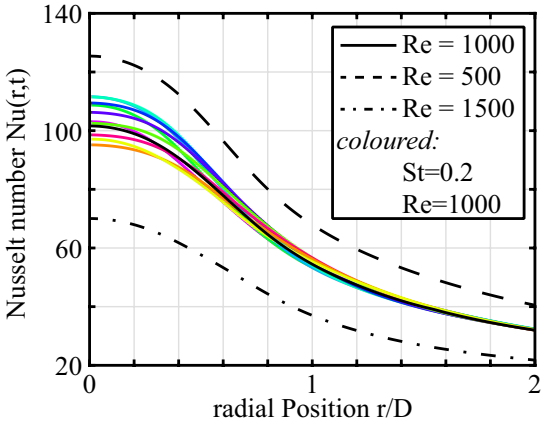

Figure 3: Nusselt number distribution over radial position, for non-pulsating (black lines), instantaneous Nusselt number distributions for a pulsating jet St=0.2 (coloured lines).

the higher deviations in the Nusselt number in the case of the slower pulsating jet are related to higher deviations of the wall shear stress.

This indicates, that at higher pulsation frequencies, the shear stresses in the boundary layer close to the wall dampens the effect of the fluctuating velocity of the flow further away from the wall. The momentum of the fluid close to the wall can not follow the rapid changes in the outer flow and the velocities fluctuate less. Hence the Nusselt number shows smaller variations over time.

Concerning the heat transfer, two counteracting effects of the fluctuating velocity can be identified. In accordance with Hofmann [11] the decrease in the time averaged Nusselt number in the case of slower pulsating jets can be explained through the dependency of the Nusselt number from the Reynolds number

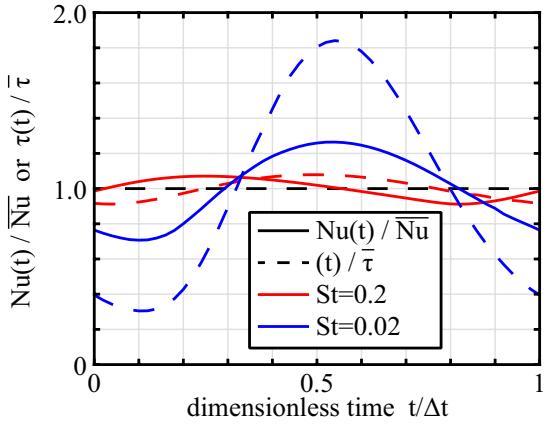

Figure 4: Variation of the stagnation point Nusselt number (solid lines) and the wall shear stress $\tau_w(r = 1 \times D, t)$ (dashed lines) each normalized by their time averaged value for a fast pulsating jet $St = 0.2$ (red) and a slowly pulsating jet $St = 0.02$ (blue).

which is generally assumed to be

$$Nu \sim Re^n \tag{9}$$

where a typical value for laminar impinging jets is $n = 0.5$. In the case of a pulsating jet, the Reynolds number is not constant but nevertheless the correlation should still apply. Compared to the Reynolds number of the non pulsating jet Re_N, the instantaneous Reynolds number of the pulsating jet Re_P as defined in equation Equation 4 fluctuates according to

$$\frac{Re_P(t)}{Re_N} = 1 + A \cdot sin(\omega t) \ . \tag{10}$$

The fraction of the time averaged local Nusselt number of the pulsating jet $Nu_P(r)$ (time averaging according to Equation 8) and the local Nusselt number of the non pulsating jet $Nu_N(r)$ can be rewritten as

$$\frac{\overline{Nu}_P(r)}{Nu_N(r)} = \frac{D \cdot q''_w \cdot \Delta t}{Nu_N(r) \cdot \lambda \int_0^{\Delta t} \theta_{w,P}(r,t) \mathrm{dt}} \tag{11}$$

$$= \Delta t \left(\int_0^{\Delta t} \frac{Nu_N(r)}{Nu_P(r,t)} \mathrm{dt} \right)^{-1} . \tag{12}$$

Neglecting other additional Reynolds number dependencies of the local Nusselt number (such as the correlation correcting nozzle-to-wall distances as suggested by Rohlfs et al. [18], in this study $H/D \cdot \overline{Re} = 4 \times 10^{-3}$), the fraction of the instantaneous Nusselt numbers in Equation 12 can be defined as

$$\frac{Nu_N(r)}{Nu_P(r,t)} = \left(\frac{Re_N}{Re_P(t)} \right)^n = (1 + A \cdot sin(\omega t))^{-n} \tag{13}$$

yielding a scaling law for the instantaneous Nusselt number of a pulsating jet

$$\frac{\overline{Nu}_P(r)}{Nu_N(r)} = \Delta t \left(\int_0^{\Delta t} (1 + A \cdot sin(\omega t))^{-n} \mathrm{dt} \right)^{-1} . \tag{14}$$

This equation indicates that the decrease in Nusselt number only depends on the relative pulsation amplitude A but is independent from the pulsation frequency ω. Assuming a scaling exponent of $n = 0.5$, the integral can be evaluated for a relative pulsation amplitude $A = 0.5$ to be

$$\frac{\overline{Nu}_P(r)}{Nu_N(r)} = 0.948 \ . \tag{15}$$

For a slowly pulsating jet, the flow in the boundary layer and hence the local instantaneous heat transfer show a quasi stationary behaviour defined by the instantaneous Reynolds number of the impinging jet. Hence the time averaged Nusselt number can be expected to be the time average of the fluctuating instantaneous Nusselt numbers as derived in Equation 10-15.

A contrary effect is caused by the increased time averaged momentum of the pulsating jet compared to the non pulsating jet. The fraction of the time averaged momentum flux of the pulsating jet $\bar{\dot{P}}_P$ defined as

$$\bar{\dot{P}}_P = \int_0^{\Delta t} \left(\int_0^{D/2} 2\pi \cdot \rho \cdot r \cdot (u_{in}(r,t))^2 \mathrm{dr} \right) \mathrm{dt} \tag{16}$$

and a non pulsating jet of the same average Reynolds number $\dot{P}_N$ is

$$\frac{\bar{\dot{P}}_P}{\dot{P}_N} = \frac{1}{\Delta t} \int_0^{\Delta t} (1 + A \cdot sin(\omega \cdot t))^2 \mathrm{dt} \ . \tag{17}$$

Hence, a non pulsating "reference" jet with the same time averaged momentum as a pulsating jet has an increased Reynolds number $Re_{N,ref}$

$$\frac{Re_{N,ref}}{Re_N} = \left(\frac{1}{\Delta t} \int_0^{\Delta t} (1 + A \cdot sin(\omega \cdot t))^2 \mathrm{dt} \right)^{0.5} \tag{18}$$

and also an increased local Nusselt number (similar to Equation 13)

$$\frac{Nu_{N,ref}(r)}{Nu_N(r)} = \left(\frac{1}{\Delta t} \int_0^{\Delta t} (1 + A \cdot sin(\omega \cdot t))^2 \mathrm{dt} \right)^{0.5 \cdot n} \tag{19}$$

which can be further reduced to

$$\frac{Nu_{N,ref}(r)}{Nu_N(r)} = \left(1+\frac{A^2}{2}\right)^{0.5\cdot n} . \tag{20}$$

For a pulsation amplitude of $A = 0.5$ and a scaling exponent $n = 0.5$ Equation 20 yields

$$\frac{Nu_{N,ref}(r)}{Nu_N(r)} = \frac{\overline{Nu}_P(r)}{Nu_N(r)} = 1.030 . \tag{21}$$

Similar to Equation 14, Equation 20 shows no dependency of the result on the pulsation frequency.

For fast pulsating jets, the flow in the boundary layer and hence the heat transfer shows a minimal fluctuation over time (see Figure 3 and Figure 4). Accordingly the shear stresses inside the boundary layer are more affected by the time averaged inertia of the outer jet. Hence the velocity profiles as well as the local heat transfer is more similar to a non pulsating jet with an increased Reynolds number according to Equation 18. This leads to an increase in local Nusselt number as calculated in Equation 21.

It should also be noted that the increase in momentum leads to an increase in time averaged pumping power that is required to achieve such a pulsating jet. The increase in required power is equal to the value of Equation 17 which yields an increase of $\approx 12.5\,\%$.

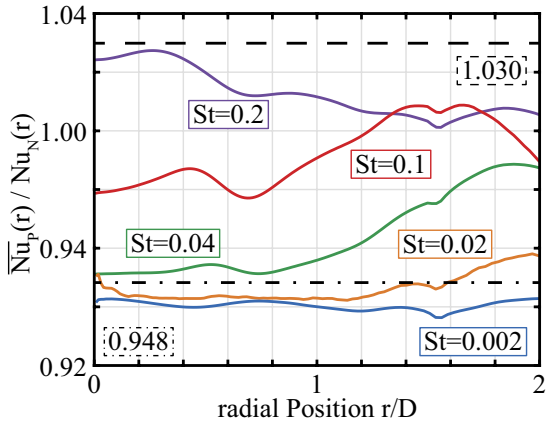

Figure 5: Fraction of the local Nusselt number distribution of pulsating jets $0.002 \leq St \leq 0.2$ over the Nusselt distribution of a non pulsating jet with the same time averaged Reynolds number; $\overline{Re} = 1000$, $Pr = 7$. The dashed lines show the bounding values calculated according to Equation 15 and Equation 21.

Figure 5 compares the local time averaged Nusselt number distribution of pulsating jets of varying pulsation frequencies ($0.002 \leq St \leq 0.2$) with the local Nusselt number distribution of a non pulsating jet of the same time averaged Reynolds number $\overline{Re} = 1000$, $Pr = 7$. Additionally the bounding values for slowly pulsating jets according to Equation 15 and a fast pulsating jet according to Equation 21 are featured (dashed lines).

Similar to the graph in Figure 1, a distinct trend is present within the stagnation region where the local time averaged Nusselt number depends on the pulsation frequency of the impinging jet. The featured bounding values derived in Equation 15 and Equation 21 seem to be valid, although the Nusselt number distribution of the two slowest pulsating jets run slightly below the lower bound. This could be explained by the simple approach to the Reynolds number dependency of the Nusselt number. More complex approaches or more exact values for the scaling exponent n might yield an even better result. Nevertheless it can be concluded that for lower pulsation frequencies local time averaged Nusselt numbers seem to tend towards a lower bound which is close to the predicted value according to Equation 15.

For higher Strouhal numbers but the bounding value derived in Equation 21 holds up as well. Though it should be noted that the changes between the local distribution for the higher Strouhal numbers is still well observable. At even higher pulsation frequencies jet breakup occurs, rendering the analytical derivations invalid. The shift between the two counteracting regimes occurs for Strouhal numbers between $St = 0.02$ and $St = 0.2$, which is a common value of interest in oscillating flows. Outside the stagnation region ($r/D > 1$) the effect of the pulsation number seems to diminish or even invert. It can be deduced that at this positions other effects, such as surface wave formation play a significant role.

It should be noted that the analytical derivations in this study can only be applied for fluid-flows with Prandtl numbers $Pr > 1$ where the thermal boundary layer is smaller than the viscous boundary layer. For lower Prandtl numbers, the flow outside the viscous boundary player plays a stronger role in the heat transfer and has to be considered as well.

CONCLUSION

The influence of flow pulsation on the heat transfer in laminar free-surface impinging jets was shown and two dominant regimes one for slowly and one for fast pulsating jets were identified. For slowly pulsating jets ($St \leq 0.02$) the heat transfer in the stagnation region, represented by the time averaged Nusselt number (see Equation 8), is reduced by about $6\,\%$ compared to values of a non pulsating jet with the same time averaged Reynolds number (see Equation 3). An analytical solution was presented (see Equation 15) to estimate this value which predicts the reduction to be $5.2\,\%$. For fast pulsating jets ($St \geq 0.2$) the heat transfer is increased by $1-3\,\%$ which was also estimated by a second analytical solution (see Equation 21) which predicts an increase by $3\,\%$. The shift between both regimes occurs at Strouhal numbers between $0.02 \leq St \leq 0.2$.

References

[1] Cho H. H., Kim K. M. and Song J., Applications of impingement jet cooling systems, *Cooling Systems: Energy Engineering and Applications*, pp. 37–67, 2011

[2] Zuckerman N. and Lior N., Jet impingement heat transfer: Physics, correlations, and numerical modeling, *Adv. Heat Transfer*, vol. 39, pp. 565–631, 2006

[3] Kneer R., Haustein H. D., Ehrenpreis C., Rohlfs W., Flowstructures and heat transfer in submerged and free laminar jets, *International Heat Transfer Conference, Kyoto, Japan*, Paper No. IHTC15-KN28, 2014

[4] Jambunathan K., Lai E., Moss M. A. and Button B. L., A review of heat transfer data for single circular jet impingement, *International Journal of Heat and Fluid Flow*, vol. 13, pp. 106-115, 1992

[5] Dewan A., Dutta R. and Srinivasan B., Recent Trends in Computation of Turbulent Jet Impingement Heat Transfer, *Heat Transfer Engineering*, vol 33, pp. 447-460, 2012

[6] Ma C. F., Gan Y. P., Tian Y. C. and lei D. H., Liquid Jet Impingement Heat transfer with or without Boiling, *Journal of Thermal Science*, vol. 2, pp. 32-49, 1992

[7] Rohlfs W., Haustein H. D., Garbrecht O. and Kneer R., Insights into the local heat transfer of a submerged impinging jet: Influence of local flow acceleration and vortex-wall interaction, *International Journal of Heat and Mass Transfer*, vol. 55, pp. 7728-7736, 2012

[8] Rohlfs W., Jörg J., Ehrenpreis C., Rietz M., Haustein H. D., Kneer R., Flow Structures and Heat Transfer in Submerged Laminar Jet Impingement., *Proceedings of the 1st Thermal and Fluids Engineering Summer Conference, ASTFE Digital Library. Begel House Inc.*, 2015

[9] Liu T., Sullivan J. P., Heat transfer and flow structures in an excited circular impinging jet, *International Journal of Heat and Mass Transfer*, vol. 39, pp. 3695-3706, 1996

[10] Chung Y. M., Luo K. H., Unsteady heat transfer analysis of an impinging jet, *ASME Journal of Heat Transfer*, vol. 124.6, pp. 1039-1048, 2002.

[11] Hofmann H. M., Wärmeübergang bei pulsierenden Prallstrahlen, *pH.D. thesis, Univ.-Verlag Karlsruhe*, 2005

[12] Zumbrunnen D. A., Aziz M., Convective heat transfer enhancement due to intermittency in an impinging jet, *Journal of Heat Transfer*, vol. 115.1, pp. 91-98, 1993

[13] Sheriff H. S., Zumbrunnen D. A., Effect of flow pulsations on the cooling effectiveness of an impinging jet, *Journal of Heat Transfer*, vol. 116.4, pp. 886-895, 1994

[14] Sabelberg E., Cardenas M., Kneer R., Rohlfs W., Design, development, and validation of concepts for generating passive pulsation in cooling nozzles, *Case Studies in Thermal Engineering*, vol. 7, pp. 103-108, 2016

[15] White F.M., Viscous Fluid Flow, second ed., *McGraw-Hill, New York*, Ch. 3–8, 1991

[16] Liu X., Gabour L.A. and Lienhard V J.H., Stagnation-point heat transfer during impingement of laminar liquid jets: analysis including surface tension, *Journal of Heat Transfer*, vol. 119 (1), pp. 99–105, 1993

[17] Weller H.G., Tabor G., Jasak H., Fureby C., A tensorial approach to computational continuum mechanics using object-oriented techniques, *Computers in Physics*, vol. 12, pp. 620-631, 1998

[18] Rohlfs W., Ehrenpreis C., Haustein H.D., Kneer R., Influence of viscous flow relaxation time on self-similarity in free-surface jet impingement, *International Journal of Heat and Mass Transfer*, vol. 78, pp. 435-446, 2014

[19] Mladin E. C., Zumbrunnen D. A., Nonlinear dynamics of laminar boundary layers in pulsatile stagnation flows, *Journal of Thermophysics and Heat Transfer*, vol. 8.3, pp. 514-523, 1994